Dependency of SAR Image Structure Descriptors with Incidence Angle

Corneliu Octavian Dumitru
Remote Sensing Technology Institute (IMF)
German Aerospace Center (DLR)
Oberpfaffenhofen - Wessling, Germany
corneliu.dumitru@dlr.de

Mihai Datcu
Remote Sensing Technology Institute (IMF)
German Aerospace Center (DLR)
Oberpfaffenhofen - Wessling, Germany
mihai.datcu@dlr.de

Abstract— **The interpretation of the structure in Synthetic Aperture Radar images depends by the used parameters and incidence angle. The evaluation is done on the high resolution SAR data and the interpretation is realized automatically. In this paper, we propose to study and asses the behavior of the primitive feature extracted methods for images of the same scene with 2-3 look angles covering the min-max range of the sensor. The tests are done on TerraSAR-X products High Resolution Spotlight mode at 3 m resolution and two sites were found that are appropriate for this. To identify the best features and appropriate incidence angle for them the Support Vector Machine and as a measure of the classification accuracy the precision –recall were considered. The precision-recall was computed first for all investigated features and after that the best were taken into account for the incidence angle evaluation.**

Keywords - TerraSAR-X products; inicidence angle; patch; features; semantic; classification; precision-recall.

I.   INTRODUCTION

The specific information in High Resolution (HR) SAR (Synthetic Aperture Radar) images acquired in single polarization is mainly in the "structure", e.g. textures, objects, or scattering signatures. The "spatial context" becomes very important rather then the "pixel based" descriptors which are less informational. The adopted solution is to analyze image patches corresponding to ground areas of ca. 200x200m. Experiments and tests carried recently confirmed the usefulness of the concept, however further analysis is needed to asses the behavior of the method for the indexing of very large SAR data sets as the case in Image Information Mining (IIM).

There are few publications available [1] ÷ [5] where the images are tile into patches. In [1], the patch size is 256x256 m in order to ensure that the extracted information capture the local characteristics within a patch rather the global features across the entire image.

In [2], the TerraSAR-X (TSX) HR Spotlight products (resolution of ~1 m) were tiled into patches of 200x200m in order to characterize the large and relatively small structures available in the urban scene. The images covered different region: Las Vegas, Venice, Gizah, and Gauting.

In [3], the original images are tiled into patches of 16x16 pixels or 128x128 pixels. The results of the classification (city, forest, and sea) were better for the patch size of 128x128 pixels. The same authors propose in [4] a patch

contextual approach for HR satellite images (resolution of 0.6 m) where the patch size is 200x200 pixels.

In our previous work [5], a pyramid with different resolutions (1m, 2m, 2.9m, 4m, and 8m) was considered for TSX HR Spotlight where each image was tiled into patches at different size in order to have the same area cover on the ground. The patch sizes vary from 400x400m (for 1m resolution) to 25x25m (for 8m resolution).

The paper structure is the following. Section 2 presents the TSX products used for tests, while Section 3 explains the actual state-of-the-art of the feature extraction methods and shortly describe the applied methods. Section 4 provides the details about the experiments and points the conclusion. The references end the paper.

II.   TERRASAR-X PRODUCTS

TerraSAR-X is the German radar satellite launched on June 2007. It operates in the X-band and is a side-looking SAR based on active phased array antenna technology. It does supply high quality radar data for purposes of scientific observation of the Earth [6].

The basic products are available in a huge diversity of modes (Stripmap, Spotlight, ScanSAR), types (complex, detected, geocoded), and configurations (Spatially Enhanced Products or Radiometrically Enhanced Products) [6].

For our investigation, we considered TSX products, geocoded product, high resolution spotlight mode, and radiometrically enhanced. Two sites are downloaded from the TSX EOWEB portal [7], one covering the Berlin area and the second one the Ottawa area. For these two sites the parameters extracted from the metadata of each product are: Berlin-the ground range resolution is about 2.9m, the orbit direction with ascending looking, and the incidence angles are 30° and 42°, and Ottawa-the ground range resolution is similar, but the orbit direction is descending and the incidence angles are 27°, respectively 41°.

The number of looks depends by the incidence angle and varies from 5 for an incidence angle of 20° to 9 for an incidence angle of 55°.

III.   FEATURES EXTRACTION METHODS

Many feature extraction methods have been proposed in the past several decades but few authors are compare these feature for satellite images.

On a conceptual level we decide which features can be extracted in general and on a practical level, we apply the: gray level co-occurrence feature extraction [33] for texture

analysis, Gabor filtering [18] to extract any geometrical or neighbourhood relationships, quadrature mirror filters [30] for texture analysis, and non-linear short time Fourier transform [32] for spectral characteristics of the image.

We can divide the features in two categories: statistical and spectral.

A. Statistical

1) Gray level co-occurrence matrix

a) State of the art

The gray level co-occurrence matrix (GLCM) is a second order statics of how often different combinations of pixel brightness values (gray levels) occur in an image [13].

Haralick et al. [8] compute gray level co-occurrence matrix for a distance of one with four directions (0°, 45°, 90°, and 135°). For a seven-class classification problem, they obtained approximately 80% classification accuracy using texture features in remote sensing images application.

Rignot and Kwok [9] have analysed SAR images using texture features computed from GLCM. However, they supplement these features with knowledge about the properties of SAR images. For example, image restoration algorithms were used to eliminate the specular noise present in SAR images in order to improve classification results.

Schistad and Jain [10] compare different methods for texture computation in ERS SAR imagery. One of the used and computed methods was GLCM with four directions like in [8]. The *angular second moment, contrast, entropy, cluster shade, inertia, and inverse difference moment* [13] were computed as texture features from the GLCM. A five class classification problem was considered and 29% (an average) classification error using GLCM was obtained.

Randen and Husoy [11] consider GLCM as a reference method and they compared this with other filtering methods (like: QMF, Gabor, discrete cosine transform, etc) for texture extraction. The size of the gray levels in the image is 8 x 8 (also chosen by Ohanian and Dubes [12]). On the one hand, if the value is large, the number of pixel pairs contributing to each element in image will be low, and the statistical significance poor. On the other hand, if the gray levels are low, much of the texture information may be lost in the image quantization. The *angular second moment, contrast, correlation, and entropy* were computed as texture features for each orientation. The average of the classification error was 32%.

b) Applied method

The GLCM is created from a gray scale image by selecting either horizontal (0°), vertical (90°), or diagonal (45° or 135°) orientation.

The size of GLCM depends on the number of gray values available in the image. For example, in [29], they obtain for an input image of 8 bits, i.e., 256 values, a GLCM of 256x256 elements.

In our case, we scale the radiometric range of the input images to 16 steps and obtain a GLCM size of 16x16 elements.

The texture parameters [33] computed from the GLCM are: *mean, variance, entropy, contrast, energy, correlation,* *homogeneity, autocorrelation, dissimilarity, cluster shade, cluster prominence,* and *maximum probability*.

B. Spectral

1) Gabor filters

a) State of the art

A Gabor filter (GAFS) is a linear filter used in image processing.

Randen and Husoy [11] review the major filtering approaches to texture feature extraction and performed a comparative study by comparing with two classical non-filtering approaches (GLCM which is a statistical method and autoregressive which is model based method). The dyadic Gabor filter bank (i.e. Gaussian shaped band-pass filters, with dyadic coverage of the radial spatial frequency range and multiple orientations) proposed by Jain and Farrokhnia [14] was considered for the experiments in [11]. Five radial frequency were used (proposed by [14] for images of size 256 x 256 pixels) and four orientations (0°, 45°, 90°, and 135°). The average error on the classification was 31%.

Du [15] used texture features derived from Gabor filters to segment SAR images. He successfully segmented the SAR images into categories of water, new forming ice, older ice, and multi-year ice. Lee and Philpot [16] also used spectral texture features to segment SAR images.

Shu et al. [17] extract the information at four directions (0°, 45°, 90°, and 135°) by using Gabor filters and then computing the mutual information of each corresponding image pair. The experiments show that the method can work very well even if the SAR image is not filtered; this indicates that the method is robust to speckle noise.

In Manjunath and Ma [18] a Gabor wavelet based texture analysis method is proposed and its application to image databases is demonstrated on Brodatz texture database but also considering the current work related to the idea of browsing large satellite images database. The experiments results demonstrate that these Gabor features are robust. Rotation and scale invariance are important in many applications and the preliminary results obtained by [18] using Gabor features are very promising.

In [19] ÷ [22], the Gabor filters are applied to Brodatz texture database with very good results.

b) Applied method

Frequency and orientation representations of a Gabor filter are similar to those of the human visual system, and it has been found to be particularly appropriate for texture representation and discrimination. In the spatial domain, a 2D Gabor filter is a Gaussian kernel function modulated by a sinusoidal plane wave [18]. The Gabor filters are self-similar - all filters can be generated from one mother wavelet by dilation and rotation.

We have chosen the Gabor filters designed by Manjunath and Ma at Vision Research Lab, University of California.

The texture parameter results computed from the Gabor filter are *mean* and *variance* for different *scales* and *orientations*.

2) Quadrature mirror filters

a) State of the art

Quadrature Mirror Filter (QMF) banks are multirate (i.e. with variable sampling rate throughout the system) digital filter banks, introduced by Croisier, [23], Esteban and Galand [24]. During the last two decades since the inception of QMF banks, they have been extensively used in speech signal processing, image processing and digital transmultiplexers [25]. QMF banks are used to split a discrete-time signal into a number of bands in the frequency domain to process each sub-band in independent manner.

QMF was used for texture analysis by Randen and Husoy [11] as extended classes of filters which include among others Gabor filters, discrete cosine transform, etc. This is a large class of filters which incorporate both infinite impulse response (IIR) and finite impulse response (FIR) filters. In their experiments the average of the classification error was between 26% and 33%.

b) Appplied method

As proposed in [30], statistical features obtained from the filtered images using QMF banks in synergy with some other features can be used for image (satellite image) indexing.

The number of features which can be obtained from the presented algorithm depends upon the level selected for the QMF sub-band decomposition like a wavelet. Features are nothing but the mean and variance of the four filtered and sub-sampled images in the QMF sub-band pyramid.

There are many techniques available to design QMF banks. We have chosen the QMF banks designed by Simoncelli and Adelson at the Vision Science Group, The Media Laboratory, MIT [34].

The parameters computed from the QMF banks (QMFS) are *mean* and *variance* of the *low pass sub-band*, *horizontal sub-band*, *vertical sub-band*, and *diagonal sub-band*.

3) Non-linear short time Fourier transform

a) State of the at

Much work on extraction of features based on short time Fourier transform is done in speech and audio processing.

The method proposed in [26] was investigated by Li and Ogihara [32] for music information retrieval. They are using short time Fourier transform feature extraction method to extract the timbral texture witch is not capture by the popular method in speech and music processing, the Mel-frequency cepstral coefficients. The derived features computed from STFT are: spectral centroid, spectral Rolloff, spectral flux, low energy, and zero crossings.

The goal of Popescu et al. paper [26] is to define an analysis model for High Resolution Spotlight SAR imagery, which is able to integrate the radiometric, as well as geometric and texture properties of the SAR data, in order to facilitate large data-base queries by informational content indexing of the images. The proposed model use the information contained in the spectra of the SAR signal.

The Short Time Fourier Transform (STFT) was considered in order to extract the features necessary for the Bayesian Support Vector Machine classifier. The features are: spectral centroid, spectral flux, cepstral coefficients, and first and second statistic measures. Using this method a number of 30 classes were recognized from the 9,000 patches of SAR images acquired with TerraSAR-X satellite.

b) Appplied method

This method of SAR image feature extraction and complex image information retrieval was first proposed in [31]. This non-parametric analysis is a form of time frequency analysis where the cutting of a spectrum allows the study of the phase responses of scatterers seen from different viewing angles.

The STFT extracts six non-linear features: the first two features are based on statistical properties of the spectrum and the next four features are timbre features used for music genre classification [32].

Non-linear STFT (NLFT) features were initially proposed mainly for feature extraction from complex-valued SAR images, but experiments showed that they give very encouraging results also for real-valued images.

Our proposed algorithm is an implementation of the non-linear STFT feature extraction. The features parameters computed from the STFT are: *mean* of the STFT coefficients, *variance* of the STFT coefficients, *spectral centroid in range*, *spectral centroid in azimuth*, *spectral flux in range*, and *spectral flux in azimuth*.

IV. PERFORMANCE EVALUATION

Presently Earth Observation (EO) satellites acquire huge volumes of high resolution images, very much over-passing the capacity of the users to access the information content of the acquired data. In addition to the existing methods for EO, data and information extraction are needed new methods and tools to explore and help to discover the information hidden in large EO image repositories.

For our investigation two sites were considered: Berlin-Germany and Ottawa – Canada. For the evaluation of the best features the Berlin site was considered in order to compute the precision-recall of GLCM, GAFS, QMFS and NLFT features. After the best features were identified these are used for answering to the question "Which is the best incidence angle". In this case both sites, Berlin and Ottawa were process.

To evaluate the feature extraction methods and the best incidence angle a tool based on Support Vector Machine with relevance feedback (SVM – RF) was built.

The SVM – RF tool supports users to search images (patches) of interest in a large repository. The Graphical User Interface of this tool allows Human-Machine Interaction to rank the automatically suggested images which are expected to be grouped in the class of relevance. Visual supported ranking allows enhancing the quality of search results by giving positive and negative examples as right and left click respectively.

The size of the images covering the area of: Berlin is 5549x3368 pixels and Ottawa the size is 4783x3381 pixels.

In our case, the product-image is tile in patches with the size of 220x220m, and after that, sub-sampled to 110x110m for better performances (see in [5] the comparison results).

The feature vector for GLCM has a fix number of features for each orientation equal to 12 features, but in our

experiments all the orientations (from 1 to 4) were considered obtaining a feature vector of 48 features (denoted by GLCM_1_2_3_4). In the case of Gabor filters, 4 scales and 6 orientations (48 features denoted by GAFS 4_6) were considered. For QMFS, the number of levels of wavelet decomposition was equal to 1 this means a vector of 8 features was obtained (denoted by QMFS 1), while for NLFT the number of features was fixed to 6.

All the features are normalised before being used in the SVM-RF tool. For normalisation the Z-score normalisation method was selected from the many available and used [33].

We define a number of semantic classes and group the patches accordingly, using the SVM-RF tool and the human expertise. In our approach, for assigning the patches into classes, one patch was assigned only to one class based on the dominant content of the patch.

During the evaluation, the number of classes retrieved for Berlin area is 11 classes and for Ottawa area the number of classes is 6 (some examples are shown in Figure 1).
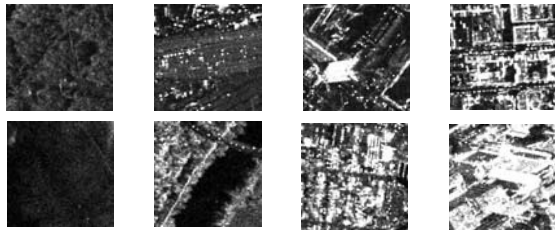

Figure 1. Typical classes extracted from the Berlin image (first line) and from Ottawa (second line).

For each feature extraction method, we tried to detect the classes among the number of identified patches of our database. For each class, we give 20% of the patches of each class for the training as positive examples and one patch from the rest of the classes as a negative example and we tray to detect the similar patches during 7-10 training iterations. The evaluations stop when the classified patches which are displayed by the Search Engine (SVM - RF tool) remain in a stable result. The procedure is repeated two times for the same class, giving the same positive and negative examples in the same order.

For the quantitative assessment, we compared the classification results with the annotated database. We purpose for our evaluation the Precision-Recall that will be computed for each class, feature, and incidence angle.

The precision is defined as the fraction of the retrieved images which are relevant, while the recall is defined as the fraction of relevant images which have been retrieved.

For the evaluation of the best feature that are intend to be used for the evaluation of the incidence angles, in Table I and Table II are displayed (for Berlin site with 30° of the incidence angle) the precision-recall for all four features, each class separately. With red colour is marked the best result obtained for each class, with blue colour is represented the average of the precision or recall for each class or feature algorithm, and with green colour is represented the global average of the precision or recall for entire product-mode-patch (this means for all investigated classes and feature algorithms).

After the investigation and comparison between the features is done the following observation arise:

a) The Gabor filters perform better than the other features especially when the precision is computed.

b) Regarding the recall, the best performance is obtained for quadrature mirror filters.

c) The quadrature mirror filters has the advantage of being faster (in required run time for feature computation) than the Gabor filters.

Based on the previous remarks, for evaluating the best incidence angle the GAFS and QMFS are taking into account. The two selected feature extraction methods were applied for this investigation to our dataset (Berlin and Ottawa).

On the TerraSAR-X archive [6], we identified two sites with different incidence angles and orbit direction: Berlin 30° and 42° with ascending looking and Ottawa 27° and 41° with descending looking.

In the next tables (Table III –IV), for these two sites the precision-recall was computed and the results are displayed. With blue color is represented the average of the precision or recall for each class or feature algorithm and with green color is represented the global average of the precision or recall for entire mode-incidence angle. The best incidence angle was obtained for both sites in the case of bigger value of the incidence angle.

We are focus only to recall because is more relevant than the precision for our investigation.

TABLE I.   THE PRECISION- COMPARISON BETWEEN ALL PF ALGORITHMS (GEC-RE PRODUCT, SPOTLIGHT MODE AND PATCH SIZE 110X110) - BERLIN

Semantics	Class No	GAFS 4_6	GLCM 1_2_3_4	NLFT	QMFS 1	Average features - class
Forest	class00	100.00%	100.00%	73.33%	81.25%	88.65%
Forest + other objects	class01	84.62%	75.76%	76.79%	79.69%	79.22%
Channel	class02	100.00%	92.59%	70.73%	63.16%	81.62%
Train lines type 1	class03	100.00%	100.00%	100.00%	100.00%	100.00%
Urban type 1	class04	86.37%	86.67%	90.91%	68.97%	83.23%
Train lines type 2	class05	100.00%	100.00%	100.00%	100.00%	100.00%
Building reflection	class06	80.10%	65.45%	53.09%	61.25%	64.97%
Urban type 2	class07	100.00%	60.00%	36.84%	65.22%	65.52%
Street plus building	class08	58.33%	75.00%	20.00%	55.00%	52.08%
Urban type 3	class09	81.82%	71.43%	68.75%	90.00%	78.00%
Sport fields	class10	100.00%	100.00%	100.00%	100.00%	100.00%
Average all class / features		**90.11%**	**84.26%**	**71.86%**	**78.59%**	*Total: all classes and features: 81.21%*

TABLE II.   THE RECALL - COMPARISON BETWEEN ALL PF ALGORITHMS (GEC-RE PRODUCT, SPOTLIGHT MODE AND PATCH SIZE 110x110) - BERLIN

Semantics	Class No	GAFS 4_6	GLCM 1_2_3_4	NLFT	QMFS 1	Average features - class
Forest	class00	71.43%	71.43%	78.57%	92.86%	78.57%
Forest + other objects	class01	66.67%	75.76%	65.16%	77.27%	71.22%
Channel	class02	51.35%	67.57%	78.38%	64.86%	65.54%
Train lines type 1	class03	58.33%	66.67%	66.67%	58.33%	62.50%
Urban type 1	class04	63.33%	50.00%	66.67%	66.67%	61.67%
Train lines type 2	class05	27.27%	27.27%	63.64%	63.64%	45.46%
Building reflection	class06	68.06%	50.00%	59.72%	68.06%	61.46%
Urban type 2	class07	32.35%	26.47%	20.59%	44.12%	30.88%
Street plus building	class08	14.58%	31.25%	25.00%	22.92%	23.44%
Urban type 3	class09	32.15%	35.71%	39.29%	32.15%	34.83%
Sport fields	class10	55.56%	55.56%	44.44%	55.56%	52.78%
Average all class / features		**49.19%**	**50.70%**	**55.28%**	**58.77%**	*Total: all classes and features: 53.49%*

TABLE III.   THE PRECISION / RECALL - COMPARISON BETWEEN DIFFERENT INCIDENCE ANGLES (GEC-RE PRODUCT WITH SPOTLIGHT MODE) - BERLIN

Semantics	Class No	Precision		Recall	
		Incidence angle = 30°	Incidence angle = 42°	Incidence angle = 30°	Incidence angle = 42°
		Average features - class		Average features - class	
Forest	class00	100.00%	90.63%	64.29%	82.15%
Forest + other objects	class01	95.17%	82.16%	81.82%	71.97%
Channel	class02	98.08%	81.58%	60.81%	58.11%
Train lines type 1	class03	100.00%	100.00%	41.67%	58.33%
Urban type 1	class04	88.46%	77.67%	58.34%	65.00%
Train lines type 2	class05	100.00%	100.00%	41.67%	45.46%
Building reflection	class06	83.09%	70.68%	42.36%	68.06%
Urban type 2	class07	82.36%	82.61%	32.35%	38.24%
Street plus building	class08	66.59%	56.67%	29.17%	18.75%
Urban type 3	class09	89.59%	85.91%	32.15%	32.15%
Sport and other fields	class10	100.00%	100.00%	44.45%	55.56%
Total all classes and features		*91.21%*	*84.35%*	*48.10%*	*53.98%*

TABLE IV.   THE PRECISION/RECALL - COMPARISON BETWEEN DIFFERENT INCIDENCE ANGLES (GEC-RE PRODUCT WITH SPOTLIGHT MODE) - OTTAWA

Semantics	Class No	Precision		Recall	
		Incidence angle = 27°	Incidence angle = 41°	Incidence angle = 27°	Incidence angle = 41°
		Average features - class		Average features - class	
Water	class00	100.00%	92.19%	70.97%	79.04%
Channel	class01	97.62%	89.58%	65.63%	67.19%
Building reflection	class02	87.97%	79.79%	59.53%	80.96%
Urban type 1	class03	98.17%	96.24%	66.67%	76.07%
Urban type 2	class04	100.00%	68.00%	59.38%	62.50%
Field	class05	88.10%	85.16%	88.10%	66.67%
Total all classes and features		*95.31%*	*95.31%*	*68.38%*	*72.07%*

V.   CONCLUSION

Based on the presented results and the parameters of the TSX products extracted from the XML file, a general conclusion can be drawn that, for value of the incidence angle closer to the upper bound of the sensor range (for TerraSAR-X High Resolution Spotlight mode products the bounds are around 20° for lower value and 55° for upper value) combined with orbit orientation (ascending or descending looking) give better results that in the case when the value of the incidence angle is closer to the lower bound of the sensor range.

For Berlin this is 42° and for Ottawa is 41°. For these two sites the number of retrieved classes is equal to 11 for Berlin area and to 6 for Ottawa area.

The good classes in recall are: for Berlin – forest, forest plus other objects, building reflection and urban; for Ottawa – water, channel, building reflection, urban, field. (2) The bad classes in recall are only for Berlin - street plus building class.

REFERENCES

[1] C.-R. Shyu, M. Klaric, G. Scott, A. Barb, C. Davis, and K. Palaniappan, "GeoIRIS: Geospatial Information Retrieval and Indexing System – Content Mining, Semantics Modeling, and Complex Queries", IEEE Trans. Geoscience and Remote Sensing, vol. 45, Issue 4, pp. 839-852, 2007.

[2] A. Popescu, I. Gavat, and M. Datcu, "Image Patch Contextual Descriptors for Very High Resolution SAR data: A Short Time Fourier Transform Non-Linear Approach", "in press".

[3] P. Birjandi and M. Datcu, "ICA based visual words for describing under meter high resolution satellite images", Proc. of. IGARSS 2009, Cape Town, 2009.

[4] P. Birjandi and M. Datcu, "Patch Contextual Descriptors for Very High Resolution Satellite Images: A Topographic ICA Approach", "in press".

[5] C.O. Dumitru, J. Singh, and M. Datcu, "Selection of relevant features and TerraSAR-X products for classification of high resolution SAR images", EUSAR 2012, May 2012.

[6] TerraSAR-X: "Basic Products Specification Document", Issue: 1.6 (TX-GS-DD-3302), April 2012.

[7] https://centaurus.caf.dlr.de:8443/eoweb-ng/template/default/welcome/entryPage.vm, April 2012.

[8] R. M. Haralick, K. Shanmugam, and I. Dinstein, "Textural features for image classification", IEEE Trans. Systems, Man, and Cybernetics, SMC-3, pp. 610-621, 1973.

[9] E. Rignot and R. Kwok, "Extraction of Textural Features in SAR Images: Statistical Model and Sensitivity", Proc. International Geoscience and Remote Sensing Symposium, Washington, DC, pp. 1979-1982, 1990.

[10] A.S. Solberg and A. Jain, "Texture Fusion and Feature Selection Applied to SAR Imagery", IEEE Trans. Geoscience and Remote Sensing, vol. 35, no. 2, pp. 475-478, 1990.

[11] T. Randen and J.H. Husoy, "Filtering for Texture Classification: A Comparative Study", IEEE Trans.Pattern Analysis and Machine Intelligence, vol. 21 no.4, pp. 291-310, 1990.

[12] P.P. Ohanian and R.C. Dubes, "Performance Evaluation for Four Classes of Textural Features", Pattern Recognition, vol. 25, no. 8, pp. 819-833, 1992.

[13] http://www.fp.ucalgary.ca/mhallbey/orderliness_group.htm, April 2012

[14] A.K. Jain and F. Farrokhnia, "Unsupervised Texture Segmentation Using Gabor Filters", Pattern Recognition, vol. 24, no. 12, pp. 1167-1186, 1991.

[15] L. J. Du, "Texture Segmentation of SAR Images Using Localized Spatial Filtering", Proc. International Geoscience and Remote Sensing Symposium, Washington, pp.1983-1986, 1990.

[16] J. H. Lee and W. D. Philpot, "A Spectral-Textural Classifier for Digital Imagery", Proc. International Geoscience and

[17] L. Shu, T. Tan, M. Tang, and C. Pan, "A Novel Registration Method for SAR and SPOT Images", Proc. IEEE International Conference on Image, pp. II.213-II.216, 2005.

[18] B. S. Manjunath and W. Y. Ma, "Texture Features for Browsing and Retrieval of Image Data". IEEE Trans. Pattern Analysis and Machine Intelligence, vol.18, pp.837–842, 1996.

[19] P. Porter and N. Canagarajah, "Robust Rotation-Invariant Texture Classification: Wavelet, Gabor filter and GMRF based Schemes", Proc. Visual Image Processing, vol. 144, no. 3, pp. 180-188, 1997.

[20] S.E. Grigorescu, N. Petkov, and P. Kruizinga, "Comparison of Texture Features based on Gabor Filters", IEEE Trans. Image Processing, vol. 10, no. 11, pp. 1160-1167, 2002.

[21] D. Zhang, A. Wong, M. Indrawan, and G. Lu, "Content-based Image Retrieval Using Gabor Texture Features", IEEE Trans. Pattern Analysis and Machine Intelligence, pp. 13-15, 2000.

[22] M. Torres-Torriti and A. Jouan, "Gabor vs. GMRF Features for SAR Imagery Classification", Proc. Int. Conference on Image Processing, Thessaloniki, vol. 3, pp. 1043 – 1046, 2001.

[23] A. Croisier, D. Esteban, and C. Galand, "Perfect Channel Splitting by use of Interpolation/Decimation/Tree Decomposition Techniques", Proc. International Conference on Information Science and Systems, Patras Greece, 1976.

[24] D. Esteban and C. Galand, "Application of quadrature mirror filters to split-band voice coding schemes", Proc. IEEE Int. Conf. ASSP, Hartford, Connecticut, pp. 191-195, 1977.

[25] P. Vaidyanathan, "Quadrature Mirror Filter Banks, M-band Extensions and Perfect-Reconstruction Techniques", IEEE ASSP Magazine, vol. 4, no. 3, pp. 4-20, 1987.

[26] A. Popescu, C. Patrascu, I. Gavat, J. Singh, and M. Datcu, "Spotlight TerraSAR-X Data Modeling using Spectral Space-Variant Measures, for scene Targets and Structure Indexing", Proc. The 8th European Conference on Synthetic Aperture Radar, Aachen, Germany, 2010.

[27] T. Zou, W. Yang, D. Dai, and H. Sun, "Polarimetric SAR Image Classification Using Multifeatures Combination and Extremely Randomized Clustering Forests", EURASIP Journal on Advances in Signal Processing vol. 2010, ID 465612, 9 pages, 2010.

[28] M. Fauvel, J. Chanussot, J.A. Benediktsson, and J.R. Sveinsson, "Spectral and Spatial Classification of Hyperspectral Data using SVMs and Morphological Profiles", IEEE International Geoscience and Remote Sensing Symposium, Barcelona, Spain, pp. 4834-4837, 2002.

[29] R. Haralick, K. Shanmugam, and I. Dinstein, "Textural Features for Image Classification", IEEE Trans. Systems, Man, and Cybernetics, vol. 3, no. 6, pp. 610–621, 1973.

[30] M. Campedel, E. Moulines, and M. Datcu, "Feature Selection for Satellite Image Indexing", ESA-EUSC: Image Information Mining – Theory and Application to EO, 2005.

[31] A. Popescu, I. Gavat, and M. Datcu, "Complex SAR image characterization using space variant spectral analysis", Proc. IEEE Radar Conference, pp. 1-4, 2008.

[32] Z. Li and M. Ogihara, "Towards Intelligent Music Information Retrieval", IEEE Trans. Multimedia, vol. 8, no. 3, pp. 564-574, 2006.

[33] N. Karthikeyani Visalakshi and K. Thangavel, "Impact of Normalization in Distributed K-Means Clustering". Int. Journal of Soft Computing, vol. 4, no. 4, pp. 168-172, 2009.

[34] http://persci.mit.edu/pub_pdfs/simoncelli_subband.pdf, April 2012.